ChemComm

Unexpected high binding energy of CO2 on CH3NH3PbI3 lead-halide organic-inorganic perovskites via bicarbonate formation

Journal:	*ChemComm*
Manuscript ID	CC-COM-06-2018-004749.R1
Article Type:	Communication

Journal Name

COMMUNICATION

Unexpected high binding energy of CO_2 on $CH_3NH_3PbI_3$ lead-halide organic-inorganic perovskites via bicarbonate formation

Received 00th January 20xx,
Accepted 00th January 20xx

DOI: 10.1039/x0xx00000x

www.rsc.org/

M. T. Nayakasinghe,[a] Y. Han, [a] N. Sivapragasam,[a] D. Kilin, [a]* and U. Burghaus [a]*

The adsorption kinetics of CO_2 was experimentally characterized in ultra-high vacuum (UHV). Unexpectedly, large desorption tempera-tures (640 K, 170 kJ/mol) were seen. Density functional theory (DFT) calculations suggest the stabilization mechanism: bicarbonate formation in the defected perovskite film due to CO_2 and H_2O coadsorption.

So-called lead-halide organic-inorganic perovskites are currently a much debated new material for solar-to-electric power conversion, LASER, light emitting diodes, photodetectors, etc.[1-5] Advantages of these new materials include low-cost solution-based fabrication, high power conversion efficiencies (>20%), direct band gaps, long charge carrier diffusion lengths, low carrier effective masses, high absorption coefficients, wide range of light-absorption, and high extinction coefficients. However, problematic is the long-term materials/device stability affected by an intrinsic thermal degradation[4] and the sensitivity to ambient gases (moisture, CO_2, etc.) of the perovskites.[6] The stability of the material has already been studied in detail before,[6-11] but mostly at ambient conditions (i.e. in air) or in solution, using optical spectroscopy and chemical engineering type experimental techniques. In this project, we study the effect of adsorbed CO_2 and water using surface science techniques at UHV conditions combined with DFT calculations. CO_2 and water are present in the ambient and therefore problematic for any real-world applications. Also, CO_2 is in the focus of scientific attention due to its environmental impact and possible utilization as a feedstock for the chemical industry; both CO_2 and H_2O are standard probe molecules in surface science.[12-17] Large CO_2 desorption temperatures, as high as 640 K, were seen on $CH_3NH_3PbI_3$ polycrystalline thin film samples, indicative of very unusual kinetics and rare CO_2 surface chemistry on the perovskite. Note that molecular physisorbed/ chemisorbed CO_2 usually desorbs well below about 300 K on basically any known planar surface (metals, metal oxides, sulphides, carbides, semiconductors, alloys, etc.);[12-16] however, similarly large desorption temperatures have been reported for a porous MgO material.[18] DFT calculations, conducted directly as part of this project, revealed a subtle combination of chemical and morphological effects resulting in such stable adsorption state of CO_2. According to DFT, CO_2 and H_2O form adsorbed carbonic acid (H_2CO_3) or bicarbonate (HCO_3^-) which is trapped inside of a defected perovskite structure. CO_2 adsorption on/in the perovskite leads to much smaller binding energies. In addition, CO_2 adsorption destabilizes the perovskite to some extent. The results are scientifically interesting since carbonic acid/bicarbonate formation as a (sub)surface reaction is rather unusual for CO_2 chemistry.

We used a typical ambient pressure solution-based procedure commonly described in the literature[3, 6] to fabricate polycrystalline perovskite thin films, namely drop casting (spin coating) of a precursor solution (which is 40 wt. % methylammonium triiodo plumbate $[CH_3NH_3]^+[PbI_3]^-$ in dimethylformamide) on indium doped tin oxide glass (ITO) in a flow of dry N_2. (This support also is often used in devices;[7] for synthesis details see ESI, Fig. S1/S2.) The simplicity of this fabrication process is the major advantage for applications in photovoltaics. The as-prepared samples were immediately transferred to a UHV chamber and/or placed into a N_2 filled storage container. Samples transferred to UHV were degassed in UHV at temperatures up to 380 K. Higher degassing temperatures destroy the samples; ion sputtering for cleaning cannot be used on these thin film samples. Thus, sample cleaning is limited, but the UHV environment prevents further accidental adsorption of contaminations as well as allows for application of surface science measuring techniques. Data collected from numerous different films are shown since these samples easily decomposed or changed irreversibly during the course of our experiments. Only few UHV surface science studies were so far conducted on lead-halide organic-inorganic perovskites mostly concerning the characterization of the material[4, 19] and thin film growth.[20, 21] Gas-surface interactions have apparently not been considered in any detail at UHV with surface science techniques.

Plane waves DFT calculations were performed with the Vienna Ab initio Simulation Package (VASP)[22-25] using projected augmented wave potentials and generalized gradient approximation with Perdew-Burke-Ernzerhof exchange-correlation functional including semiempirical pairwise corrections and spin-orbit coupling. The atomic models were represented by a cross-section of the orthorhombic perovskite with the (001) surface on top.[26] The supercell consisted of 96 atoms composed of alternating

[a] *Department of Chemistry and Biochemistry, North Dakota State University (NDSU), Fargo, ND 58108, USA.*
* uwe.burghaus@ndsu.edu; dmitri.kilin@ndsu.edu
URL http://www.uweburghaus.us/
† Footnotes relating to the title and/or authors should appear here.
Electronic Supplementary Information (ESI) available: [Experimental details, additional data]. See DOI: 10.1039/x0xx00000x

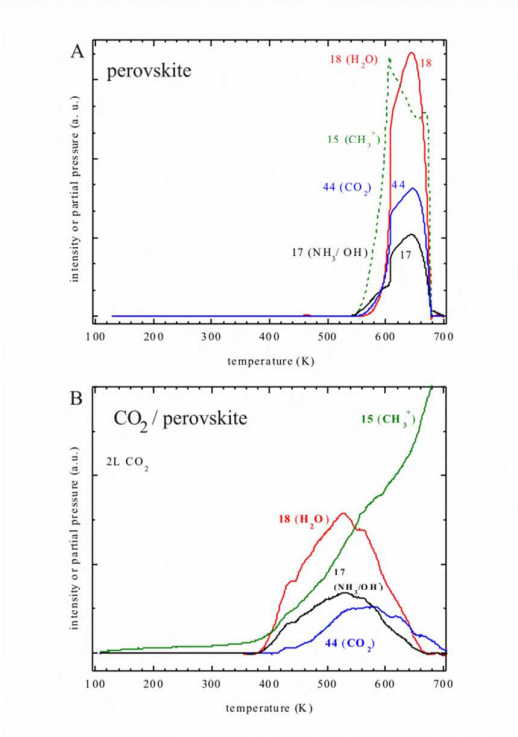

Fig. 1: A) Multi-mass thermal desorption spectroscopy (TDS) of an as-prepared perovskite thin film sample; **B)** TDS after a 2L dose of CO_2 on a 2nd sample.

stoichiometric sublayers of lead iodide and methylammonium iodide: 4* $(CH_3NH_3)_2Pb_2I_6$) = 4* (2 (PbI_2) + 2 (CH_3NH_3) I) with periodic boundary conditions imposed in each direction and a 15 Å vacuum spacing layer normal to the surface (described as $(CH_3NH_3)_8Pb_8I_{24}$). In addition, a defect structure was constructed by removing a surface $CH_3NH_3^+$ cation and I^- in the second PbI_2 layer (described as $(CH_3NH_3)_7Pb_8I_{23}$ see ESI for further details as well as the image of atomic model below).

Numerous experimental techniques were used to characterize the samples. UV-vis and surface thickness experiments were conducted at ambient pressure. In addition, XRD (X-ray diffraction), EDX (energy-dispersive X-ray spectroscopy), AES (Auger electron spectroscopy), and SEM (Scanning Electron Microscopy) data were collected in vacuum to characterize the samples prior to the UHV kinetics experiments; see Fig. S3-S8 in ESI. The obtained results are consistent with the literature. Experimental binding energies, E_d, were determined from the thermal desorption spectroscopy (TDS) peak positions, (with uncertainty of ±0.5 kJ/mol) using the Redhead equation. (See ESI for details.) TDS is a standard kinetics technique used in surface science where the sample temperature is increased with time and simultaneously desorbing species are detected with a mass spectrometer inside of a UHV chamber. As-prepared samples were analysed or samples that were at low temperatures pre-dosed with gases.

Fig. 1A shows the result of such a TDS experiment, i.e., depicted are the species desorbing from an as-prepared perovskite sample into UHV as a function of temperature. We recorded several different species m/e = 17, 15, 18 and 44 corresponding to NH_3 (or OH from water), CH_3, H_2O and CO_2 in the multi-mass TDS experiment. According to Fig. 1A, gas desorption and sample decomposition of a pristine sample in UHV starts above 540 K with

	System	E_d	Fig.
DFT	surface-CO_2	12	S11A
	surface-H_2O	40	S12A
	surface-H_2CO_3 [a]	53	S12B
	surface-(H_2O + H_2CO_3) [b]	121	2A
	vacancy-(H_3O^+ + HCO_3^-) [c]	166	2B
Exp.	as-received surface	170	1
	2L CO_2 on surface	153	1

[a] $E_d = E_{surface} + E_{CO_2} + E_{H_2O} - E_{surface-H_2CO_3}$
[b] $E_d = E_{surface} + E_{CO_2} + 2E_{H_2O} - E_{surface-(H_2O+H_2CO_3)}$
[c] $E_d = E_{vacancy} + E_{CO_2} + 2E_{H_2O} - E_{vacancy-(H_2O^+ + HCO_3^-)}$

Tab. 1: Theoretical (most stable configurations) and experimental (from TDS) binding energies, E_d, in kJ/mol.

TDS peak maxima within 600-640 K. No desorption was detected below 500 K. In contrast, for experiments in ambient, a decomposition temperature of 334 K was reported.[27] The greater thermal stability in UHV is plausible since the decomposition is not only caused by thermal degradation, but also by interaction with adsorbates. That the perovskite film and decomposition products mostly desorbed during the >700 K ramp is evident from AES data collected after the TDS experiment (Fig. S8). Various decomposition mechanisms are described in the literature including[6, 10] (1) $CH_3NH_3PbI_3$ → PbI_2 + CH_3I + NH_3 and (2) $CH_3NH_3PbI_3$ → PbI_2 + CH_3NH_2 + HI. Indeed, NH_3 (ammonia) is detected in favour of the first mechanism (Fig. 1). In addition, CH_3 (methyl) which is one of the mass fragments[28] in CH_3I (methyl iodide) and CH_3NH_2 (methylamine) is evident in our experiment (Fig. 1). More importantly, CO_2 and water, originally adsorbed during the ambient pressure synthesis, desorbed. AES data consistent with adsorbed PbI_2 were detected on surfaces (Fig. S8) flashed to 600 K, beyond that also lead iodide desorbs leaving a clean ITO substrate behind. Therefore, our data would be consistent with mechanism (1).

Fig. 1B depicts multi-mass TDS data from a 2nd sample after adsorption of 2 L CO_2 in UHV at ~100 K. The TDS traces are very similar to the prior case. The lower desorption temperatures reflect a greater CO_2 surface concentration after the additional CO_2 dose e.g. due to repulsive lateral interactions. Variations in the shape of the scans may reflect variations in sample morphology. Note that CO_2 seems to also destabilize thermally the perovskite film, judged by the CH_3 desorption temperatures. On the bare perovskite film the onset of CH_3 desorption is at 560 K (Fig. 1A) whereas for the CO_2 dosed perovskite desorption starts already at 400 K (Fig. 1B).

New and unexpected are the great desorption temperatures for CO_2 and water. What causes the unusual CO_2 and H_2O desorption in huge amounts above 600 K?

Regarding what is known from the literature, the CO_2 and H_2O desorption temperatures are too large for physisorbed gases. For example, physisorbed water desorbs usually below 200 K; [17, 29-32] similarly typical CO_2 physisorption binding energies are within (20-40) kJ/mol with desorption temperatures below 300 K (see e.g. Tab. 5 in ref.[13]). Assuming molecular adsorption/desorption, the TDS peak temperatures of ~640 K (Fig. 1) would correspond to a binding energy of 170 kJ/mol (using a pre-exponential of $1x10^{13}$/s, see ESI). Nearly the same binding energy is obtained for a 2nd order desorption process (using a pre-exponential of $1x10^{21}cm^2/(mol\ s)$, ref.[33]). These are unusually high binding energies and desorption temperatures. It is impossible, that water will adsorb/desorb molecularly at such high temperatures. The formation of hydroxyls or OH–H_2O clusters and recombinative desorption of these could explain greater desorption temperatures for water.[17] Molecular CO_2 binding even on metal oxides is much weaker.[13] Formation of

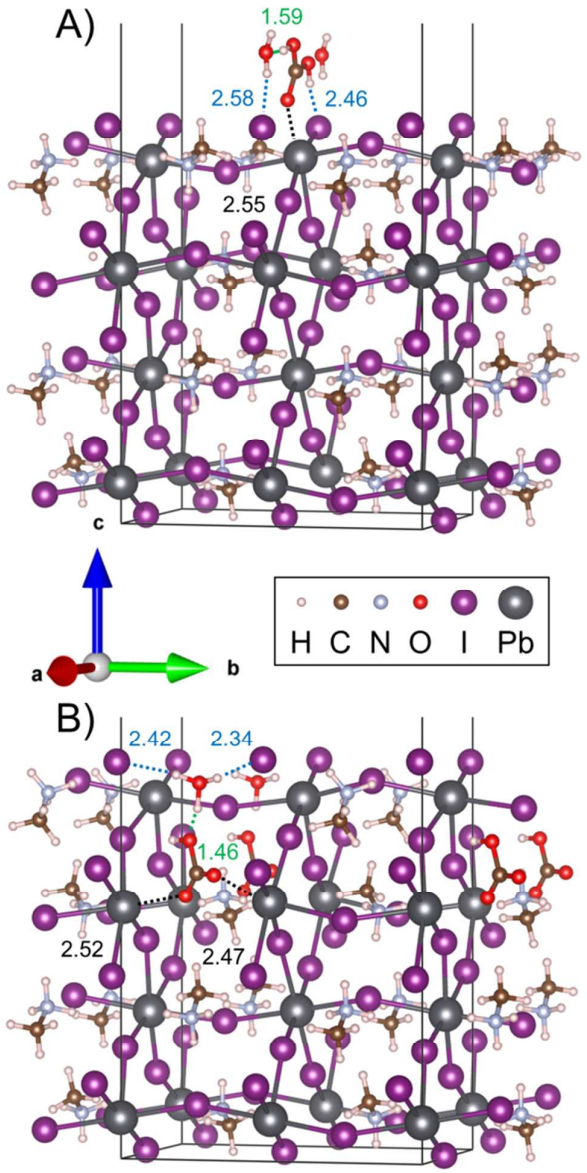

Fig. 2: Perovskite model **A)** H_2O–H_2CO_3 complex and **B)** defect structure with embedded H_3O^+ and HCO_3^-. The box represents the simulation cell. Each cell contains a H_2O–H_2CO_3 complex or H_3O^+–HCO_3^- ion pair. Additional species observed in panels A) and B) are due to visualization with periodic boundary conditions. The vacuum layers are not explicitly shown. For selected atoms, interatomic distances in Å are indicated.

carbonate-like species[13, 34] and strong (polydentate) chemisorption would be the only adsorption/reaction pathway known from the literature that could lead to similarly large desorption temperatures. For example, on CaO carbon dioxide desorption up to 500 K was seen due to formation of carbonates.[35] Carbonates are usually formed in O_2–CO_2 coadsorption phases or on O-sites of metal oxides. The perovskite film does not directly provide oxygen adsorption sites nor dissociates CO_2 for carbonate formation, but water is clearly coadsorbed (Fig. 1). CO_2 stabilization by water is known to occur in rare cases,[36, 37] however, not to the extent seen here (CO_2 desorbs at 200 K in coadsorption with water on a Pd surface via carboxylate (bent CO_2^-) formation).[36] Bicarbonates form if at all, usually in tiny amounts on surface defect sites.[34] (One of the few known examples is CO_2 + H_2O coadsorption on a defected TiO_2(110) surface, producing adsorbed HCO_3^- that desorbs as CO_2 at 213 K).[34] Carbonate binding in a polydentate chemisorption geometry, where the adsorbate interacts simultaneously with multiple surface sites would enhance binding strength and has been proposed for powder samples. (Indeed on ZrO_2 powders decomposition temperatures of ~500 K for polydentate carbonates were reported).[38] This geometry becomes more likely on inhomogeneous surfaces, consistent with the perovskite. Importantly, the perovskites do possess internal adsorption sites which also could result in larger desorption temperatures due to adsorption/desorption kinetics inside of the pores (Knudsen diffusion) or polydentate adsorption geometries. Diffusion is usually much faster than TDS temperature ramps, i.e., it unlikely affects the kinetics. Note that we did conduct various blind experiments which rule out CO_2 desorption at high temperatures from the sample holder (see Fig. S9). Given the huge binding energies, the hypothesise that several stabilization mechanisms are active simultaneously appears plausible which is quite unusual for CO_2 surface chemistry. The porous structure makes surface/subsurface reactions plausible. DFT calculations conducted directly as part of this project allowed to identify a possible mechanism.

Using DFT calculations, first, numerous surface adsorption sites for molecular CO_2 adsorption were tested; none of which resulted in binding energies even close to the experimental value (Tab. 1 and Fig. S11, S12). Next, adsorption of carbonic acid (H_2CO_3) and its coadsorption with water were considered. An increase in binding strength became evident due to multi-site interactions (polydentate adsorption) and H_2CO_3–H_2O complex formation, but still the binding energy was much lower than the experimental value. Finally, H_3O^+ and HCO_3^- embedded in a defected perovskite structure resulted in good qualitative agreement of experiment and theory (Tab. 1). Indeed, DFT confirms that unusually large binding energies for CO_2 are possible.

Quantitatively, E_d for molecular CO_2 adsorption amounts to only 12 kJ/mol, a value consistent with CO_2 physisorption,[13] but it is much smaller than the experimental value measured here. The binding energy increases to 53 kJ/mol for H_2CO_3 adsorbed on the surface. Adsorbed carbonic acid[34] could form from water and CO_2 co-adsorbed on the surface via CO_2 + H_2O → H_2CO_3. Water is clearly present on our perovskite sample made at ambient (Fig. 1) and is typical for any real-world application.

The binding energy approximately doubles and reaches 121 kJ/mol when water is co-adsorbed along with H_2CO_3, see Fig. 2A. Thus, water would assist forming carbonic acid in the first place that then further interacts with adsorbed water. That interaction gives rise to a van der Waals H_2O–H_2CO_3 complex, which provides more binding sites to the surface, increasing E_d. As a result, E_d(H_2O + H_2CO_3) is greater than E_d(H_2O) + E_d(H_2CO_3), see Tab. 1. However, the binding energy of carbonic acid and its complex with water are still distinctly smaller than the experimental values.

Therefore, we considered a defected perovskite structure consisting of a $CH_3NH_3^+$ cation vacancy, as shown in Fig. 2B. Instead of forming a molecular carbonic acid – water complex adsorbed on the surface, bicarbonate and hydronium could form according to H_2CO_3 + H_2O → HCO_3^- + H_3O^+. Here H_3O^+ and HCO_3^- are replacing the corresponding natural cation and anion of the intrinsic perovskite structure. H_3O^+ taking place of $CH_3NH_3^+$ and HCO_3^- replaces I^-, conserving the crystal structure (Fig. 2B). Similar mechanisms are known in colloidal chemistry.[39-41] In our calculations, this

configuration gives the largest binding energy of 166 kJ/mol which is actually quite close to the experimental value of 170 kJ/mol (Tab. 1). (The calculated E_d is the low coverage limit. Therefore, it should be compared with the as-prepared samples.)

This CO_2 stabilization is caused by several factors. Because the perovskite crystal structure remains intact, the intrinsic ion attraction that forms the crystal in the first place also is conserved. The bicarbonate anion replaces iodine and coordinates with divalent lead in the same way as the iodine anion was originally coordinated. Such complexation has similarity to a stable compound namely dicarboxyoxylead or $Pb(HCO_3)_2$. Also, the hydronium cation substitutes the methylammonium cation. Therefore, it becomes stabilized by neighbouring iodine anions. In addition, hydronium cation and bicarbonate anion experience electrostatic attraction to each other. The embedding of H_3O^+ and HCO_3^- in the crystal may be considered a morphological stabilization, whereas the formation of HCO_3^- would be a chemical stabilization of CO_2, as mentioned in the introduction. The entire process may be considered as a subsurface-surface reaction. (Note, however, that the active site for bicarbonate formation is just 4.5 Å below the outer surface layer formed by the I-atoms, see image in ESI. Indeed, we describe a subsurface reaction and not a bulk or solid state type process.) All of this is quite unusual for CO_2 chemistry.

The embedded HCO_3^- could indeed thermally decompose and desorb as gas phase CO_2 according to HCO_3^- (embedded) → CO_2 (gas) + OH(adsorbed) which is indeed first order kinetics in the HCO_3^- (or CO_2) concentration. Even a UHV chamber has a significant hydrogen gas residual background. Therefore, adsorbed or embedded hydroxyl could form again water according to OH(ads) + H(ads) → H_2O (ads) → H_2O (gas). Assuming that this reaction step is fast, water and CO_2 would indeed desorb simultaneously, as detected experimentally. As a parallel reaction pathway, bicarbonates could form as H_2CO_3 → HCO_3^- + H^+. The CO_2 / water induced defect structure that replaces $CH_3NH_3^+$ and I^- is consistent with the thermal destabilization of the perovskite by CO_2 adsorption mentioned above.

Conclusions

CO_2 desorption at temperatures as high as 640 K was seen on $CH_3NH_3PbI_3$ thin films. This may be compared with granular MgO based mesoporous materials[18] where desorption is seen at comparable large temperatures or with highly reactive CaO surfaces where CO_2 desorbs only within 100-450 K[35] DFT calculations suggest formation of a defect structure were H_3O^+ replaces $CH_3NH_3^+$ and HCO_3^- replaces I^- of the perovskite. As part of the mechanism, bicarbonates and carbonic acid are formed as surface/subsurface reactions of CO_2 with water. Although this is unusual CO_2 surface chemistry, the effect of water and CO_2 will regularly be encountered in technological applications of these perovskites.

Financial support by the US Department of Energy (through SC-00001717) is acknowledged by DSK as well as discussions with Amanda Neukirsch, Sergei Tretiak, and Sergei Ivanov. M.T.N. and N.S. acknowledge fellowships from NDSU.

Conflicts of interest

There are no conflicts to declare

Notes and references

1 *A. Kojima, K. Teshima, Y. Shirai and T. Miyasaka,* J. Am.Chem. Soc., 2009, **131,** 6050.
2 *M. D. Archer and A. J. Nozik,* 2008, Imperial College Press, 2008.
3 *W. Nie, et al.,* Science, 2015, **347,** 522.
4 *I. Deretzis, et al.,* Appl. Phys. Lett., 2015, **106,** 131904.
5 *M. D. Bhatt and J. S. Lee,* New J. Chem., 2017, **41,** 10508.
6 *J. Yang, B. D. Siempelkamp, D. Liu and T. L. Kelly,* ACS nano, 2015, **2,** 1955.
7 *Y. Liu, Z. A. Page, D. Zhou, V. V. Duzhko, K. R. Kittilstved, T. Emrick and T. P. Russell,* ACS Cent. Sci., 2018, **4,** 216.
8 *N. Rajamanickam, et al. ,* Nanotechnol. 2016, **27,** 235404.
9 *J. Troughton, K. Hooper and T. M. Watson,* Nano Energy, 2017, **39,** 60.
10 *E. J. Juarez-Perez, Z. Hawash, S. R. Raga, L. K. Ono and Y. Qi,* Energy Environ. Sci., 2016, **9,** 3406.
11 *G. Niu, X. Guo and L. Wang,* J. Mater. Chem. A, 2015, **3,** 8970.
12 *H. J. Freund and M. W. Roberts,* Surf. Sci. Rep., 1996, **25,** 225.
13 *U. Burghaus,* Prog. Surf. Sci., 2014, **89,** 161.
14 *U. Burghaus,* Catal. Today, 2009, **148,** 212.
15 Chapter 3, in NEW AND FUTURE DEVELOPMENTS IN CATALYSIS: ACTIVIATION OF CARBON DIOXIDE, S.L. Suib (Ed.), Elsevier, 2013
16 *W. Taifan, J. F. Boily and J. Baltrusaitis,* Surf. Sci. Rep., 2016, **71,** 595.
17 *M. A. Henderson,* Surf.Sci. Rep., 2002, **46,** 1.
18 *K. K. Han, Y. Zhou, Y. Chun and J. H. Zhu,* J. Hazardous Mat., 2012, **203-204,** 341.
19 *C. Wang, X. Liu, C. Wang, Z. Xiao, C. Bi, Y. Shao, J. Huang and Y. Gao,* J.Vac.Sci.Technol. B, 2015, **33,** 032401.
20 *L. She, M. Liu, X. Li, Z. Cai and D. Zhong,* Surf. Sci. 656, 2017, **656,** 17.
21 *X. Zhou, X. Li, Y. Liu, F. Huang and D. Zhong,* Appl. Phys. Lett., 2016, **108,** 121601.
22 *G. Kresse and J. Hafner,* Phys. Rev. B, 1993, **47,** 558.
23 *G. Kresse and J. Hafner,* Phys. Rev. B, 1994, **49,** 14251.
24 *G. Kresse and J. Furthmüller,* Phys. Rev. B, 1996, **54,** 11169.
25 *G. Kresse and J. Furthmüller,* Comput. Mater. Sci., 1996, **6,** 15.
26 *T. Baikie, et al.,* J. Mat.Che. A, 2013, **1,** 5628.
27 *B. Yang, O. Dyck, W. Ming, M. H. Du, S. Das, C. M. Rouleau and K. Xiao,* ACS Appl. Mater. Interfaces, 2016, **8,** 32333.
28 http://webbook.nist.gov/chemistry/
29 *J. Shan, A. Chakradhar, Z. Yu and U. Burghaus,* Chem. Phys. Lett., 2011, **517,** 46.
30 *M. T. Nayakasinghe, A. Chakradhar, N. Sivapragasam and U. Burghaus,* Appl.Surf.Sci., 2016, **364,** 822.
31 *A. Chakradhar and U. Burghaus,* Chemical Communications, 2014, **50,** 7698.
32 *P. A. Thiel and T. E. Madey,* Surf.Sci.Rep., 1987, **7,** 211.
33 *K. C. Waugh,* Catal. Today, 1999, **53,** 161.
34 *M. A. Henderson,* Surf.Sci., 1998, **400,** 203.
35 *E. Kadossov and U. Burghaus,* J.Phys.Chem. C, 2008, **112,** 7390
36 *R.Brosseau, T.H.Ellis and H.Wang,* Chem.Phys.Lett., 1991, **177,** 118.
37 *Q. Liu, Y. Han, J. Cai, E. J. Crumlin, Y. Li and Z. Liu,* Catal. Lett., 2018, **148,** 1686.
38 *B. Bachiller-Baeza, I. Rodriguez-Ramos and A. Guerrero-Ruiz,* Langmuir, 1998, **14,** 3556.
39 *F. Krieg, et al.,* ACS Energy Letters, 2018, 641.
40 *L.Protesescu, et al.,* Nano Lett., 2015, **15,** 3692.
41 *C. C. Stoumpos, et al.,* Chem. Mat. 2016, **28,** 2852.

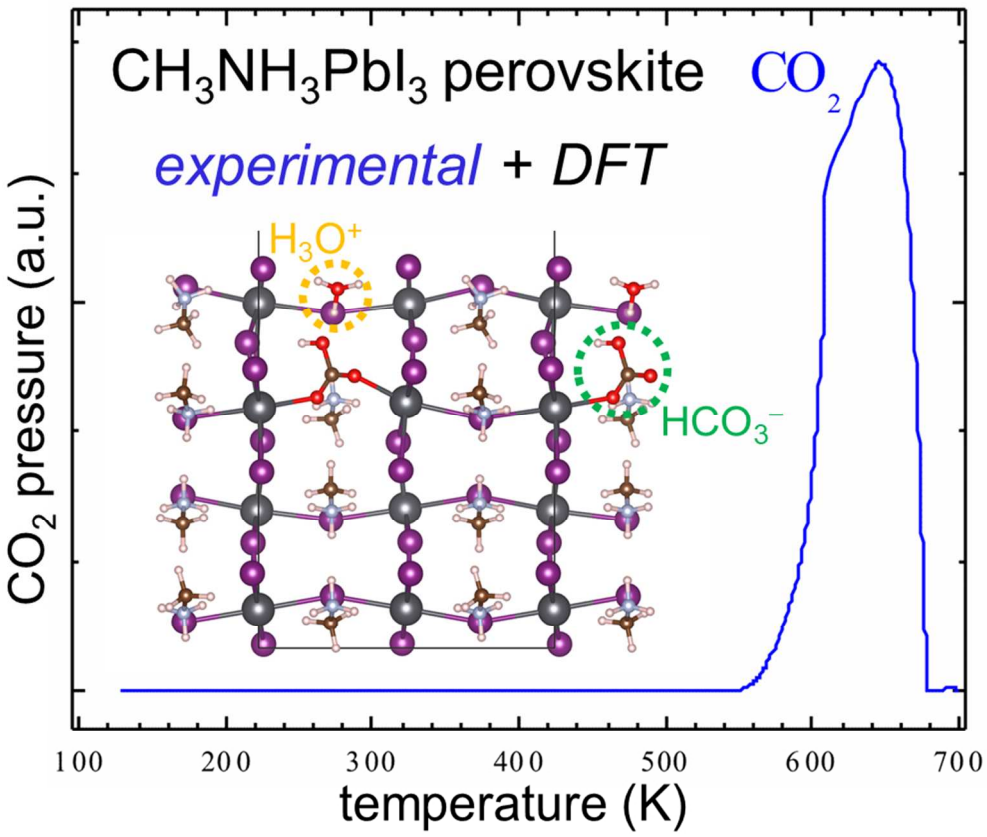

abstract figure

85x71mm (300 x 300 DPI)